Available online at http://ijcpe.uobaghdad.edu.iq and www.iasj.net
Iraqi Journal of Chemical and Petroleum Engineering
Vol.23 No.4 (December 2022) 49 – 58
EISSN: 2618-0707, PISSN: 1997-4884

Comparison of Estimation Sonic Shear Wave Time Using Empirical Correlations and Artificial Neural Network

Jassim M. Al Said Naji[a], Ghassan H. Abdul-Majeed[b], and Ali K. Alhuraishawy[c]

[a] *Petroleum Engineering Department, College of Engineering, University of Baghdad, Baghdad, Iraq.*
[b] *Department of Scientific Affairs, University of Baghdad, Baghdad, Iraq.*
[c] *Reservoir and Field Development Directorate, Ministry of Oil, Baghdad, Iraq.*

Abstract

Wellbore instability and sand production onset modeling are very affected by Sonic Shear Wave Time (*SSW*). In any field, *SSW* is not available for all wells due to the high cost of measuring. Many authors developed empirical correlations using information from selected worldwide fields for *SSW* prediction. Recently, researchers have used different Artificial Intelligence methods for estimating *SSW*. Three existing empirical correlations of Carroll, Freund, and Brocher are used to estimate *SSW* in this paper, while a fourth new empirical correlation is established. For comparing with the empirical correlation results, another study's Artificial Neural Network (*ANN*) was used. The same data that was adopted by the *ANN* study was used here where it is comprised of 1922 measured points of *SSW* and the other nine parameters of Gamma Ray, Compressional Sonic, Caliper, Neutron Log, Density Log, Deep Resistivity, Azimuth Angle, Inclination Angle, and True Vertical Depth from one Iraqi directional well. Three existing empirical correlations are based only on Compressional Sonic Wave Time (*CSW*) for predicting *SSW*. In the same way of developing previous correlations, a fourth empirical correlation was developed by using all measured data points of *SSW* and *CSW*. A comparison demonstrated that utilizing *ANN* was better for *SSW* predicting with a higher R^2 equal to 0.966 and lower other statistical coefficients than utilizing four empirical correlations, where correlations of Carroll, Freund, Brocher, and developed fourth had R^2 equal to 0.7826, 0.7636, 0.6764, and 0.8016, respectively, with other statistical parameters that show the new developed correlation best than the other three existing. The use of *ANN* or new developed correlation in future *SSW* calculations is relevant to decision makers due to a number of limitations and target *SSW* accuracy.

Keywords: Empirical correlations, artificial neural network, sonic shear wave, wellbore deviation, azimuth and inclination.

Received on 25/06/2022, Accepted on 19/07/2022, Published on 30/12/2022

https://doi.org/10.31699/IJCPE.2022.4.7

1- Introduction

Generally, sonic logs are classified alongside Density Logs (*DL*) and Neutron Logs (*NL*) as porosity logs where two types of sonic waves exist: Compressional Sonic Wave Time (CSW) and Sonic Shear Wave Time (SSW) [1]. *CSW* and *SSW* are measured either by Dipole Sonic Log (*DSI*) on site or by experiments in the laboratory by utilizing core plug samples [2] but computing *SSW* from core plug tests is an expensive and time-consuming method, and *DSI* is not running for all wells [3]. Sonic waves with density are key parameters for calculating some elastic rock mechanic properties such as Biot's coefficient, Poisson ratio, shear modulus, rock compressibility factor, and young modulus [4]. Elastic rock mechanic properties are important in geomechanical studies for prediction of wellbore instability and sand production onset [5]. Formation lithology and its properties, type of fluids that filled rocks and their properties, reservoir temperature, and hydrostatic pressure of the rock column are all parameters that affect sonic wave velocities or transmitted time. Laminated clay and structural shale content are making sonic wave transmitting time increase [6] while decreasing in water saturated rocks rather than dry rocks, where at 10% water saturated, sonic waves have a strong decrease in intensity that means an increase in wave transmitting time [7]. From the sixties of last century till now, many empirical correlations have been developed based on logs and core test data of selected worldwide reservoirs as summarized in Table **1** [8-15]. All these empirical correlations in Table 1. are developed to calculate SSW in terms of Shear Sonic Velocity (*SSV*) and Compressional Sonic Velocity (*CSV*) with velocity units of kilometer per second (km/sec), where *SSV* and *CSV* are reciprocals of *SSW* and *CSW* respectively.

Recently, at the beginning of the present century, authors have gone to work on Artificial Intelligent (*AI*) methods for estimating *SSW* because of past simple regression correlations shown in Table 1. were for special reservoir cases and did not take into account all effective *SSW* parameters. Rezaee et al. (2007) [16] applied three AI methods: fuzzy logic, neurofuzzy, and Artificial Neural Network (*ANN*) to data from two wells in the Carnarvon basin, NW shelf of Australia's sandstone reservoir, with a third well used for validation. The

Corresponding Authors: Name: Jassim M. Al Said Naji, Email: 150100@uotechnology.edu.iq, Name: Ghassan H. Abdul-Majeed, Email: ghassan@uob.edu.iq, Name: Ali K. Alhuraishawy, Email: ali19_82@yahoo.com

datasets used were Gamma Ray (*GR*), *CSV*, *NL*, Deep Resistivity Log (*DRL*), and *DL*. Tabari et al. (2012) [17] utilized the *ANN* method for predicting *SSV* by using a dataset of *GR*, *NL*, *DL*, and *CSV* of one well, while data from two wells was used for *ANN* validation. Hadi and Nygaard (2018) [18] used *ANN* for prediction of *SSV* by utilizing data from the production section in the south of Iraq where *CSV* and *DL* are used as input parameters of the input layer. Al Ghaithi and Prasad (2020) [19] adopted Feedforward Neural Network (*FNN*) for predicting *SSV* by using field data from the Norwegian North Sea where the dataset comprised *GR*, *DL*, *CSW*, *DRL*, *NL*, and Measured Depth (*MD*). Al Said Naji et al (2022) [20] on their submitted paper to the Iraqi geological journal are working on *ANN* for predicting *SSW* based on one Iraqi directional well and 1922 measured points of *SSW* that were used as the output of the proposed *ANN*, beside nine parameters of *CSW*, *GR*, *NL*, *DL*, *DRL*, Caliper (*CAL*), True Vertical Depth (*TVD*), Azimuth Angle (*AZI*), and Inclination Angle (*INC*) that utilized as inputs. They obtained the following mathematical model for SSW prediction for any directional well:

$$SSW = \sum_{j=1}^{12} W2_j \left(\frac{2}{1+e^{-2\left(W1_{j,1}\,TVD + W1_{j,2}\,CSW + W1_{j.3}\,GR + W1_{j,4}\,CAL + W1_{j.5}\,NL + W1_{j,6}\,DRL + W1_{j,7}\,DL + W1_{j,8}\,INC + W1_{j,9}\,AZI + b1_j\right)}} - 1 \right) + b2 \quad (1)$$

Where $W2_j$ is an output-hidden layers weight, $W1_{ji}$ is an input-hidden layers weights, j is the hidden layer neurons, $b1_j$ is a hidden layer biases and $b2$ represents bias of output layer.

The present study is aimed at making a comparison between utilizing three existing empirical correlations of Carroll (1969), Freund (1992) and Brocher (2005) and developing a fourth with the results of constructed ANN by Al Said Naji et al. (2022) for SSW estimation.

Table 1. Summary of Developed Empirical Correlation for *SSV* Estimation

References	Year	Correlation of SSV relation with CSV (km/sec)	Eq. number	Lithology Type
Pickett	1963	$SSV = 0.526.CSV$	(2)	Limestone
Pickett	1963	$SSV = 0.556.CSV$	(3)	Dolomite
Carroll	1969	$SSV = 0.75609.CSV^{0.81846}$	(4)	Various rock types
Castsgna, et. al	1985	$SSV = -0.05509.CSV^2 + 1.0168.CSV - 1.305$	(5)	Limestone
Freund	1992	$SSV = 0.763.CSV - 0.603$	(6)	Various rock types
Eskandari, et.al	2004	$SSV = -0.1236.CSV^2 + 1.6126.CSV - 2.3057$	(7)	Carbonate rocks
Brocher	2005	$SSV = 0.7858 - 0.1244.CSV + 0.7949.CSV^2 - 0.21238.CSV^3 + 0.006.CSV^4$	(8)	Various rock types
Ameen et al	2009	$SSV = 0.52.CSV + 0.25251$	(9)	Carbonate rocks
Al-Kattan	2015	$SSV = 0.699.CSV^{0.969}$	(10)	Carbonate rocks

- Field of Study and Reservoir Description

The Fauqi oil field is located in the Missan governorate in the south of Iraq. It is 50 km to the north–east of Ammara city and 175 km north of Basrah city, as shown in Fig. **1**. It has two domes with north-west, south-east anticlines in the north and south, respectively, and some of its northern dome stretch is in Iran. The field length is approximately 23 km and the width is approximately 7 km. The Fauqi oil field has two reservoirs: Asmari and Mishrif. Asmari is an Iranian name, and it corresponds to three Iraqi names for the reservoir, which are: Jeribe-Euphrates formation, Upper Kirkuk formation, and Middle-Lower Kirkuk formation. The Jeribe-Euphrates formation is the upper part of the Asmari reservoir that was deposited during the Neogene geological period. It is represented as an A unit with sub divisions of (A1, A2, and A3) and an average thickness of 40 m. It has a lithology that consists mainly of 85% dolomite alternated with moderately thin shale. The Upper Kirkuk formation is a middle sub-reservoir of the Asmari formation, deposited during the Paleogene geological period. It is denoted as the B unit with its classifications (B1, B2, B3 and B4) and consists basically of thick shale, alternated with thin sandstone, argillaceous limestone, calcareous shale and limestone. The sandstone portion is gray, poorly consolidated, fine to medium grained, subangular to sub-rounded, moderately sorted, predominantly quartz, and argillaceous. It has an average interval of 120 m. The Middle-Lower Kirkuk formation is a lower sub-reservoir of the Asmari formation. During the Paleogene geological epoch, the Oligocene series and stage of Aquitanian to lower Oligocene, this reservoir was deposited. It is represented as C and D units in past studies and C unit in modern studies where they are water submerged zones. Its lithology is composed mainly of thick Shale and Argillaceous Siltstone alternated with moderately thick Argillaceous Limestone and Sandstone with an average thickness of 200 m [21, 22].

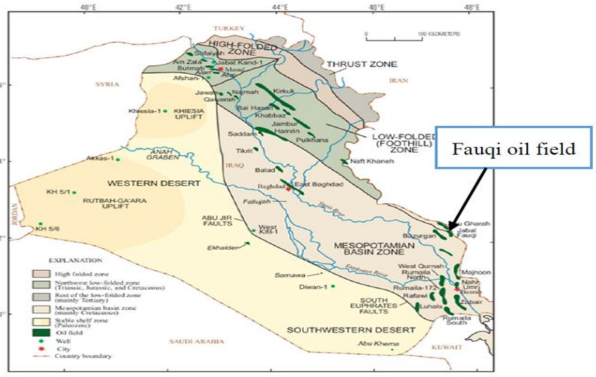

Fig. 1. Iraqi Fauqi Oil Field Location on Iraq Map [23]

2- Materials and Methods

The same dataset utilized by Al Said Naji et al (2022) [20] is used for the present paper. The selected dataset is from one directional well that penetrated the Asmari reservoir in the Iraqi Fauqi oil field. The data of the mentioned directional well is comprised of 1922 measured points of *SSW*, beside nine parameters, *CSW*, *GR*, *NL*, *DL*, *DRL*, *CAL*, *TVD*, *AZI*, and *INC*, as illustrated in Fig. **2**. As mentioned above, Al Said Naji et al. (2022) [20] used these data to construct an *ANN* for *SSW* prediction while considering the effects of well deviation parameters (*INC* and *AZI*). Eq. 1 resulted as a mathematical model of two loops to predict *SSW* for directional wells. Table **2** summarizes the used dataset of selected directional well.

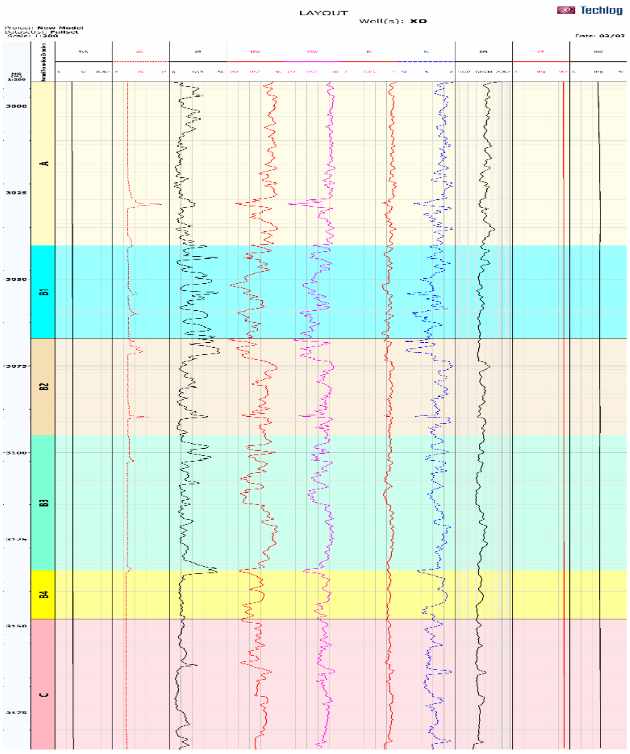

Fig. 2. Used Data of Directional Well Logs Track [20]

Table 2. Ranges Summary of Used Dataset

Parameter	Minimum	Maximum	Mean
***SSW*, (us/ft)**	89.05	156.94	112.032
***TVD*, (m)**	2993	3185.1	3089.05
***CSW*, (us/ft)**	48.58	114.3	64.09
***GR*, (GAPI)**	6.56	132.011	44.94
***CAL*, (in)**	8.43	14.698	8.77
***NL*, (dimensionless)**	0.301	44.6	16.097
***DRL*, (ohm.m)**	0.311	461.54	7.064
***DL*, (gm/cc)**	2.15	2.94	2.569
***INC*, (deg)**	44.55	48.29	47.19
***AZI*, (deg)**	321.14	323.44	322.318

2.1. Existing Empirical Correlations

Selection of an appropriate *SSW* prediction correlation for a given field is a very big challenge where any mistake in SSW estimation leads to poor prediction of rock elastic properties, making decisions on investments and losses very difficult [24]. Asmari reservoir, as described above, consists of different rock types, so any developed empirical correlation from literature based on one rock type cannot be used to calculate *SSW*. Three empirical correlations suitable for various lithology types were used to calculate *SSW* based on *CSW* data. These existing empirical correlations are Carroll (1969), Freund (1992), and Brocher (2005), illustrated in Table **1**. as Eq. 4, Eq. 6, and Eq. 8 respectively. Carroll in 1969 developed an empirical correlation for *SSV* determination by using data obtained from the volcanic region of Nevada where 62 dry core samples were collected with the same measured log data from different intervals. This correlation was established for all rock types by studying and testing the effects of lithology kinds and hydrostatical loads on *SSV* estimation [9]. Freund in 1992 established an empirical correlation based on 57, 25 and 5 samples of sandstone, siltstone, and claystone, respectively, for the well penetrated Rotliegendes reservoir in Germany. Samples had porosity ranges of 0.01–0.5 and clay content of 0.01–0.88 while measurements were made at pressure ranges between 10–300 Mpa. [11]. Brocher (2005) introduced a global empirical correlation for *SSV* determination. He used *SSV* and *CSV* datasets from various fields in California: (1) fine-grained Holocene deposits in San Francisco Bay; (2) wells with a depth of more than 410 m at Santa Clara; (3) Miocene sedimentary rocks from the central of California; (4) granodiorite and salinan terrane granites from a pilot hole at Park-field; and (5) other logs and core plugs from various fields and previous studies [13].

In this paper, the use of these three global correlations in *SSW* calculating is based on the mentioned measured data, 1922 points of *CSW*, by using Excel 2022 in the following sequence: (1) invert *CSW* to *CSV*; (2) multiply the 304.8 conversion factor to convert units from ft/us to km/sec; (3) use correlations to calculate *SSV* in units of km/sec; and (4) invert *SSV* to *SSW* and use the conversion factor to make it in units of us/ft.

2.2. Development of New Empirical Correlation

A new polynomial second order empirical correlation was developed by using the same data of *CSW* and *SSW* that consisted of 1922 measured points which used by Al Said Naji et al. (2022) [20]. This correlation is established in the same way of developing past empirical correlations mentioned in Table **1**. where its development was based on the plot in Fig. **3** below, which has the following formula with a correlation coefficient (R^2) equal to 0.8293:

$$SSW = -0.0143.CSW^2 + 3.1521.CSW - 29.73 \qquad (11)$$

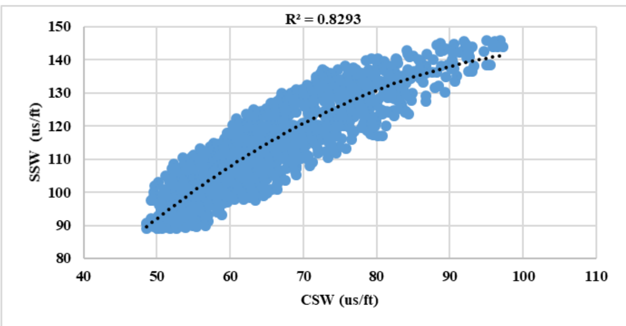

Fig. 3. Plot of Development Polynomial Second Order Empirical Correlation

2.3. Artificial Neural Network (*ANN*)

The *ANN*, constructed by Al Said Naji et al. (2022) [20] in their submitted paper to the Iraqi geological journal, is used in this study to compare with the results of utilizing three existing empirical correlations and a developed fourth. They built *ANN* by a dataset of one directional well from Iraqi Fauqi oil field with measured 1922 points of *SSW* and nine parameters of *TVD*, *CSW*, *GR*, *CAL*, *NL*, *DRL*, *DL*, *INC*, and *AZI* using MATLAB R2012b. Using multi parameters for *ANN* construction to was based on their effects on *SSW* values where some of the past literatures [2, 3, 25, 26] explained *SSW* response against different log measurements of *CSW*, *GR*, *CAL*, *NL*, *DRL*, and *DL* while Al Said Naji et al 2022 [20] on their paper demonstrated the positive impact of hole deviation parameters *INC* and *AZI* and the negative effect of *TVD* on *SSW* as summarized in Table **3**.

Table 3. Multi Logs Parameters Impact on *SSW* Prediction

Parameter	Impact on SSW Estimation
TVD	Negative
CSW	Positive
GR	Dual
CAL	Dual
NL	Positive
DRL	Negative
DL	Negative
INC	Positive
AZI	Positive

Measured *SSW* was used as a neuron of output layer while others nine parameters were entered as input layer neurons. Tangent function was adopted as hidden layer activation function as appearing in Eq. 13 while linear function showed below in Eq. 14 used for activating of output layer [27]. 1922 measured points are classified to three parts 70%, 15%, and 15% for *ANN* three processing sequences of training, validation and testing. Constructed *ANN* had optimum structure of (*ANN* 9-12-1) based on obtained maximum R^2 and minimum mean square error (*MSE*) as appear in Fig. **4** in shape of multiple layer perceptron (*MPL*) with single hidden layer. *MPL* is the popular structured of networks for functions regression that consisting from three layers input, hidden and output. Any layer contains number of neurons that connected with others of next layers with factor called weight (*W*) while another factor works on adding freedom degree in neurons connection called bias (*bi*) [28]. Each neuron of layers before hidden layer are combining and modifying by acting of hidden and output layers neurons in term of collection junction by following function [29]:

$$S_j = \sum_{i=1}^{n} X_i\, W1_{ji} + b1_j \tag{12}$$

$$f(S_j) = \frac{2}{1+e^{-2S_j}} - 1 \tag{13}$$

$$Z_P = \sum_{j=1}^{k} W2_j\, f(S_j) + b2_j \tag{14}$$

Where n is the neurons number of input layer, X_i is the input vector, $W1_{ji}$ is the weight of connection between X_i and *j*, *Sj* is the summation of input weights and biases, $b1_j$. outputs are resulting from passing of S_j though an appropriate activation function, Z_p represents estimated (*SSW*) value, $W2_j$ is an output hidden layer weight, $b2_j$ represents bias of output layer, while *k* is the neurons of hidden layer.

ANN mathematical model was obtained in Eq. 1 was by combining Eq. 12, Eq. 13 and Eq. 14 with substituting of inputs and output variables to simplify *SSW* calculations.

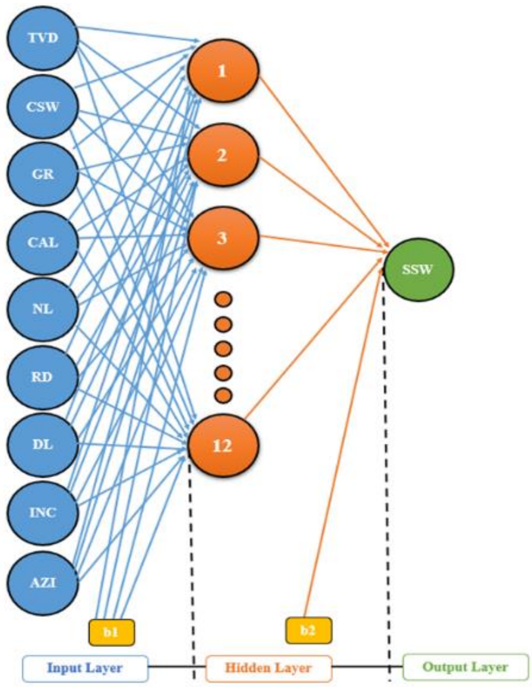

Fig. 4. *ANN* Structure for *SSW* Prediction

3- Results and Discussion

Comparison between empirical correlations and *ANN* results was based on statistical parameters of average percent error (*APE*), absolute average percent error (*AAPP*), standard deviation (*SD*), mean square error (*MSE*), and correlation coefficient R-Square (R^2) as shown in the following equations respectively:

$$APE = \frac{1}{n}\sum_{i=1}^{n}\left(\frac{Zmi - Zpi}{Zmi}\right) \tag{15}$$

$$AAPE = \frac{1}{n}\sum_{i=1}^{n}|Zmi - Zpi| \tag{16}$$

$$SD = \left(\frac{\sum_{i=1}^{n}(Z_{p,i} - Zp_{avg})^2}{n}\right)^{0.5} \tag{17}$$

$$MSE = \frac{1}{n}\sum_{i=1}^{n}(Z_{m,i} - Z_{P,i})^2 \tag{18}$$

$$R^2 = 1 - \frac{\sum_{i=1}^{n}(Z_{m,i} - Z_{Pi})^2}{\sum_{i=1}^{n}(Z_{m,i} - Zpavg)^2} \tag{19}$$

Where Z_{mi}, Z_{pi} and Z_{pavg} are measured, predicted and averaged predicted *SSW*. Fig. **5** and Fig. **6** is explaining the performance of both *ANN* and empirical correlations. As note from first looking on these two figures, *ANN* performance is better than four empirical correlations that mean applying Eq. 1 for any directional well for SSW calculation is better than using Eq. 4, Eq. 6, Eq. 8 and Eq. 11.

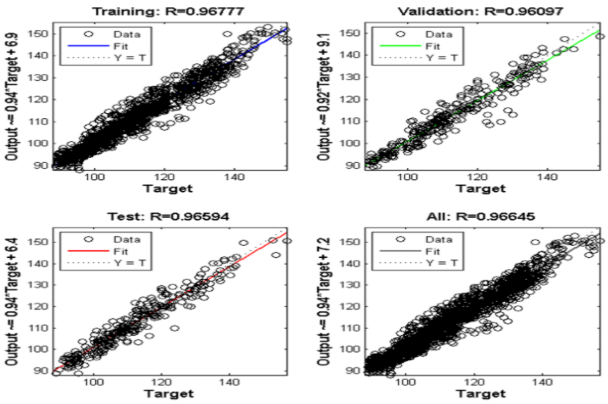

Fig. 5. *ANN* Performance Evaluation [20]

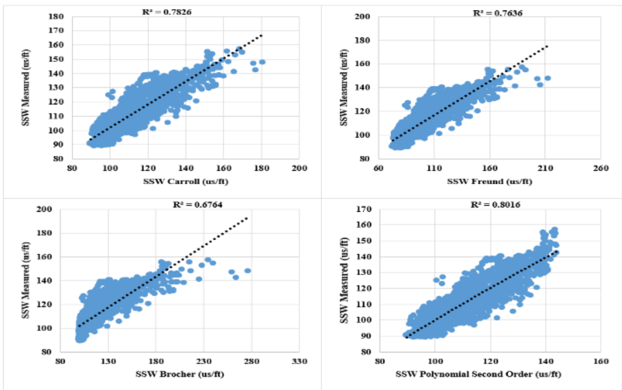

Fig. 6. Empirical Correlations Performance Evaluation

Statistical coefficients for four empirical correlations and *ANN* methods are summarized in Table **4**. as can be seen, the *ANN* approach is superior than the rest of the empirical models where it had higher R^2 and lower *APE*, *AAPE*, *MSE*, and *SD*. A new developed empirical correlation Eq. 11 is better than other existing correlations of Carroll (1969), Freund (1992), and Brcocher (2005) Eq. 4, Eq. 6, and Eq. 8 respectively.

Table 4. Statistical Parameters of SSW Prediction Methods

Model	APE	AAPE	MSE	SD	R^2
Carroll, 1969	0.29345	5.353119	50.93531	15.27	0.7826
Freund, 1992	10.03937	13.77396	239.4537	21.22	0.7636
Brocher, 2005	6.0883475	9.436357	228.8576	22.19	0.6764
Polynomial Second Order, 2022	0.16461	4.794007	38.65837	12.52	0.8016
ANN, 2022	0.006	2.168	9.62	2.69	0.966

To support the above results in Table 4., and reinforce what has been reached in the above sentences, we created the following illustrated plots. These plots: Fig. **7** presents a plot of measured and predicted *SSW* by Carroll (1969) on the X-axis with *TVD* on the Y-axis. The statistical parameters in Table **4** with this figure demonstrated that the Carroll correlation outperformed the Freund (1992) and Brocher (2005) correlations. Fig. **8** and Fig. **9** state measured *SSW* against that predicted by Freund and Brocher with *TVD*, respectively. Brocher was a bad correlation for *SSW* prediction of Asmari reservoir. Fig. **10** is applying measured and predicated *SSW* by a new developed polynomial second order correlation with *TVD*. The results show that the new developed correlation is better than the other three utilized empirical correlations, and that is expected where the new correlation was established based on measured data related to the target *SSW* of the Asmari reservoir, while others were developed by adopting data from different worldwide reservoirs that had properties different than Asmari. Fig. **11** shows the *SSW* of *ANN* with measured. Results obtained from *ANN* are much more accurate than results of other empirical methods according to account as much as possible the high number of influencing parameters on *SSW* in addition to consider wellbore deviation parameters *INC* and *AZI*. Using the *ANN* mathematical model Eq. 1 or the developed empirical correlation Eq. 11 is related to decision makers, so using the *ANN* resulted model will obtain high accuracy results of *SSW* but requires data availability and people with programming software knowledge due to the need to make two loops code for *SSW* estimation, whereas utilizing a new developed equation is easier than the *ANN* model and only requires *CSW* data but will give low accurate *SSW* prediction.

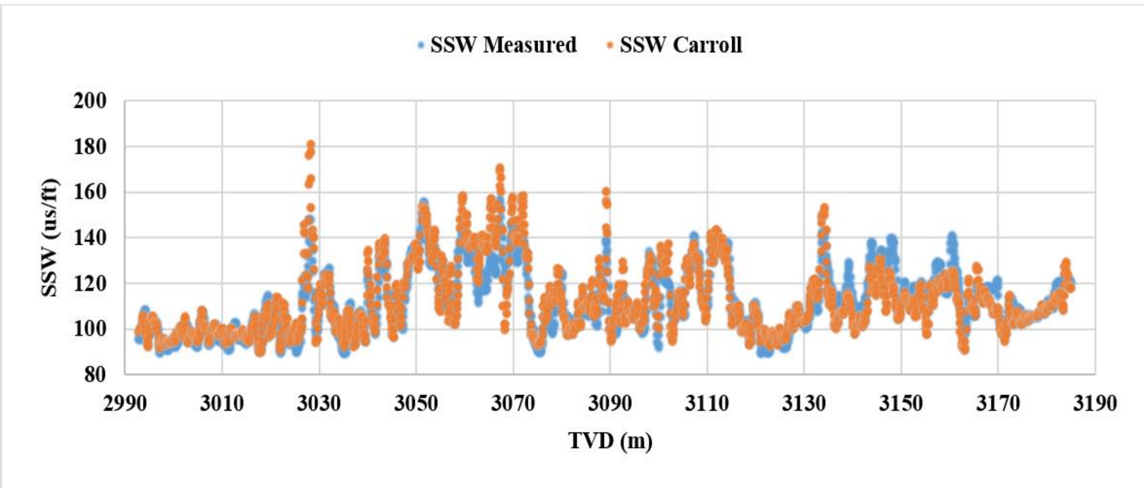

Fig. 7. Plot of Measured and Estimated SSW by Carroll Correlation with TVD

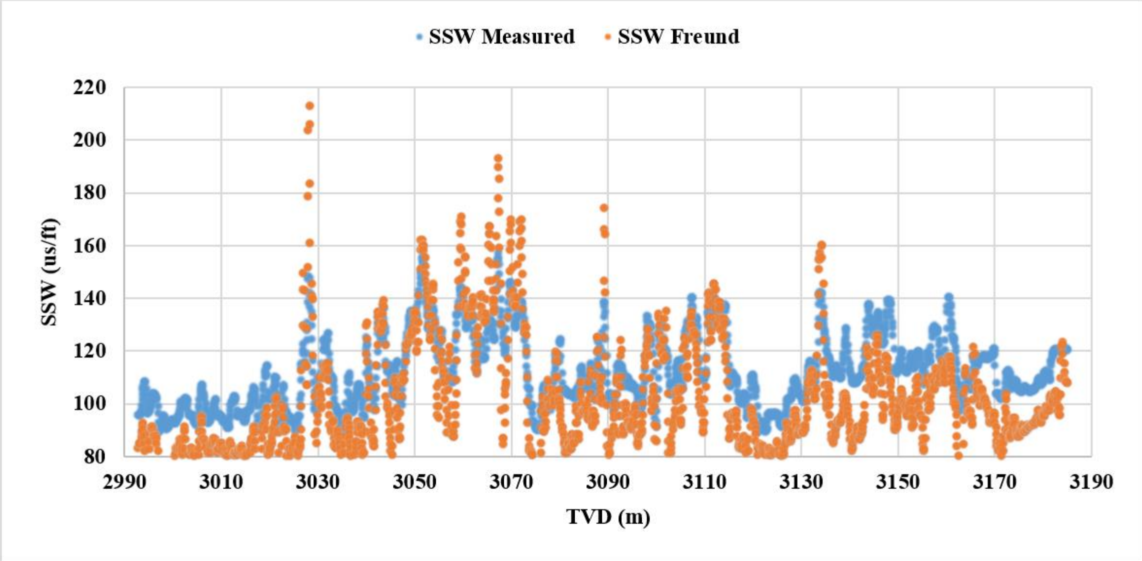

Fig. 8. Plot of Measured and Estimated SSW by Freund Correlation with TVD

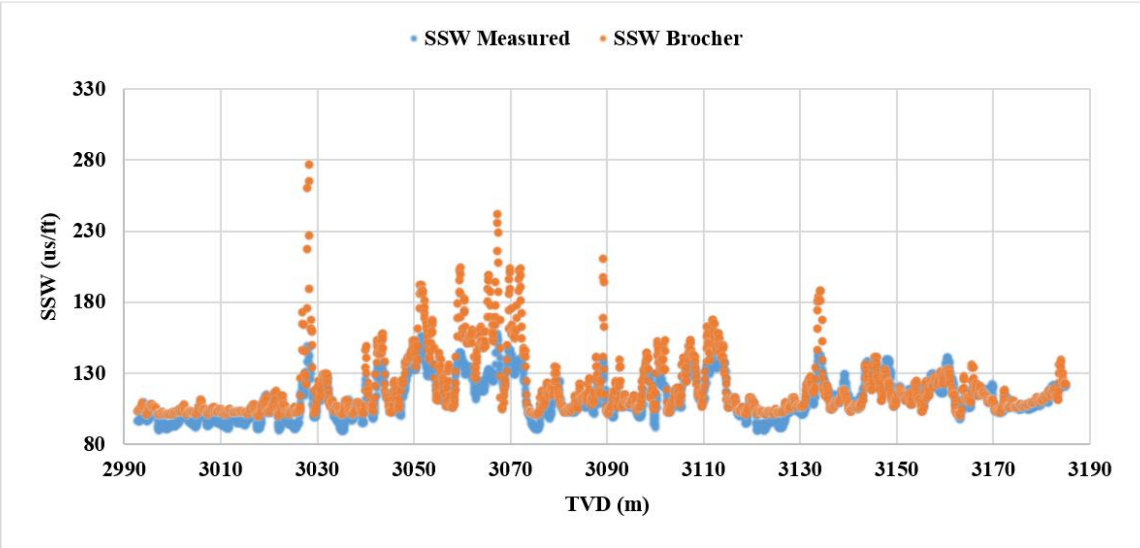

Fig. 9. Plot of Measured and Estimated SSW by Brocher Correlation with TVD

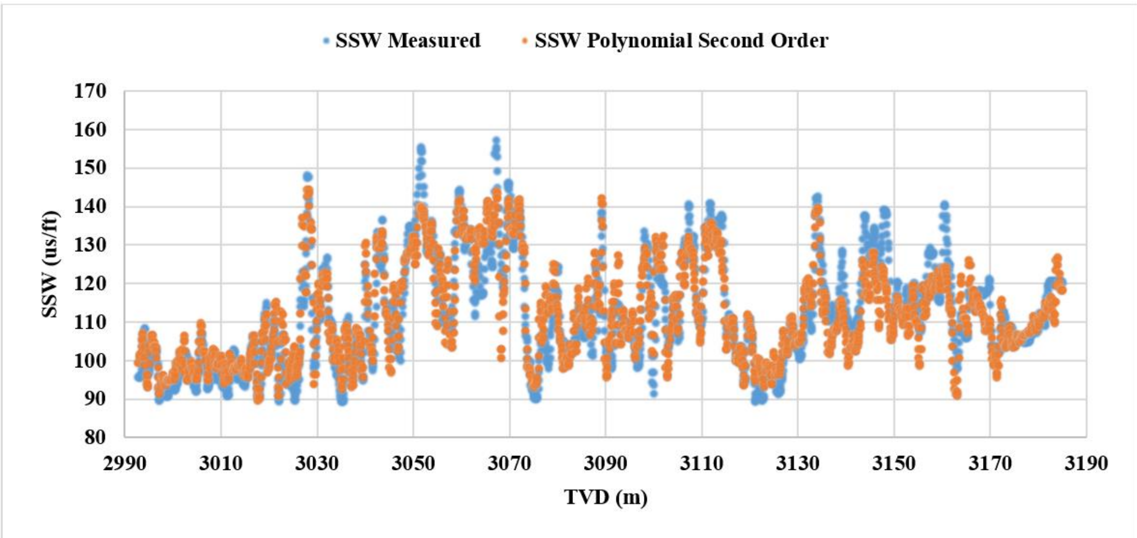

Fig. 10. Plot of Measured and Estimated SSW by Polynomial Second Order Correlation with TVD

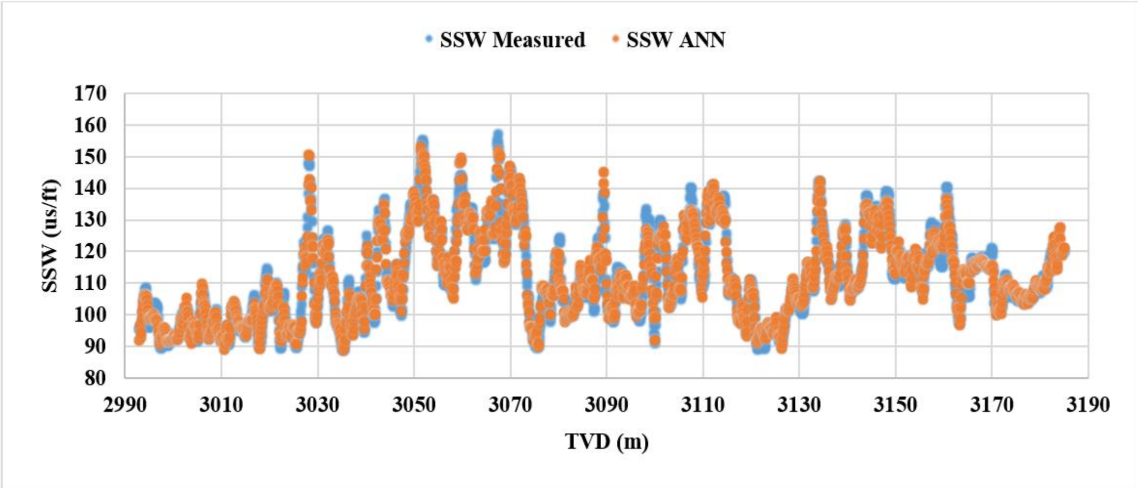

Fig. 11. Plot of Measured and Estimated SSW by ANN with TVD

To apply Eq. 1 to any directional well, use the *ANN* matrix parameters obtained by Al Said Naji et al. (2022) study in Table **5**. Constructed *ANN* was (9-12-1) in that each neuron in the hidden layer had twelve weights connected to it for each parameter in the input layer. Also, twelve weights were connected between the hidden layer neurons and the output layer neuron. Twelve biases add some degree of freedom to each neuron at the hidden layer, while a single bias supports the output layer neuron. Applying Eq. 1 using Table **5**. parameters, you need to write code for two loops to calculate SSW.

The lack of sufficient data prevented the validation of established models. We recommend validating the developed models by using data from other fields.

Table 5. Constructed ANN Matrix [20]

$W1_{j, TVD}$	$W1_{j, CSW}$	$W1_{j, GR}$	$W1_{j, CAL}$	$W1_{j, NL}$	$W1_{j, DRL}$	$W1_{j, DL}$	$W1_{j, INC}$	$W1_{j, AZI}$	$b1_j$	$W2_j$	b2
1.547	-6.385	3.107	4.66	-0.938	5.056	-4.332	1.003	1.133	3.488	-0.157	
0.603	-0.567	0.591	0.455	0.497	2.959	-0.013	0.598	-0.978	-3.935	0.583	
1.117	-1.055	2.383	19.42	-3.598	-8.034	-4.075	1.5398	-7.747	15.158	0.382	
3.7	3.088	-2.798	-1.775	3.655	-16.18	-3.027	4.316	-2.073	-19.72	0.109	
-0.709	0.2396	-0.84	-1.375	-0.565	9.056	-0.346	-0.348	0.787	7.869	-0.741	0.223
-5.465	-9.212	-5.083	7.27	3.058	6.371	-15.55	-11.23	0.752	12.453	0.0763	
-2.326	-0.749	0.991	1.715	-1.051	-3.229	-1.42	16.492	-10.83	-4.423	0.584	
-19.58	7.553	-7.6296	4.557	1.941	19.58	3.476	0.821	17.756	21.856	-0.133	
1.805	-3.608	1.336	1.612	1.311	-6.774	-1.252	-6.347	2.704	-1.796	-0.226	
1.808	3.937	-0.914	1.473	-1.629	3.678	-2.646	1.773	-8.731	0.778	0.1651	
7.043	0.634	0.949	-1.104	-1.802	-3.921	-1.334	5.821	-8.471	-4.005	0.645	
2.589	-0.912	0.643	1.908	-0.162	-1.138	-0.412	3.676	-5.105	-0.39	-1.477	

4- Conclusions

This work is presenting comparison between empirical correlations and *ANN* results for *SSW* estimation. Same dataset adopted by Al Said Naji et al 2022 is used in present study and it comprised of 1922 measured points of *SSW* with other nine parameters *TVD*, *CSW*, *GR*, *CAL*, *NL*, *DRL*, *DL*, *INC* and *AZI*. Three global existing empirical correlations of Carroll 1969, Freund 1992, and Brocher 2005 used for SSW predicting by utilizing all measured points of *CSW* from dataset. A Polynomial second order empirical correlation developed by using all measured points of *SSW* and *CSW*. *ANN* constructed by Al Said Naji et al 2022 results is used to compare with empirical correlations results. Statistical parameters demonstrated that *ANN* was very superior than others empirical correlations where it had higher R^2 and lower *APE*, *AAPE*, *MSE* and *SD*. Developed second order empirical correlation was best than other correlations of Carroll (1969), Freund (1992), and Brocher (2005) because the last were established based on worldwide fields data different than used dataset of Asmari reservoir. Using either *ANN* mathematical model equation or new developed second order empirical equation by any consequent authors will depend on data availability, persons knowledge in programming softwares and target SSW accuracy.

Acknowledgments

The authors are grateful for supporting universities of Baghdad, and Technology, Ministry of oil: petroleum

Research Develop Center and Reservoir and Development Directorate.

Nomenclature

AAPE	Absolute average percent error
ANN	Artificial neural network
APE	Average percent error
AZI	Azimuth angle (deg°)
$b1_j$	Input - hidden layers biases
CAL	Caliper log (in)
CSV	Compressional sonic velocity (ft/us) or (km/sec)
CSW	Compressional sonic wave time (us/ft)
DL	Density log (gm/cc)
DRL	Deep resistivity log (ohm.m)
DSI	Dipole sonic imager tool
FNN	Feedforward neural network
GR	Gamma ray log (GAPI)
INC	Inclination angle (dego)
j	Hidden layer neurons
MD	Measured depth (length unit)
MSE	Mean square error
n	Neurons number of input layer
NL	Neutron log (%)
R^2	Correlation coefficient
SD	Standard deviation
S_j	Summation of input weights and biases
SSV	Shear sonic velocity (ft/us) or (km/sec)
SSW	Sonic shear wave time (us/ft)
SW	Water saturation (%)
TVD	True vertical depth (m)
$W1_{ji}$	Input – hidden layer neurons connection weights
W2j	Output - hidden layer connection weights
Xi	Input vector
Zmi	Measured shear sonic wave time (us/ft)
Zp	Predicted sonic shear wave time (us/ft)
Zpavg	Average predicted sonic shear wave time (us/ft)

References

[1] H. H. Alkinani, A. T. Al-Hameedi, S. Dunn-Norman, R. E. Flori and M. A. Al-Alwani, "Intelligent Data-Driven Analytics to Predict Shear Wave Velocity in Carbonate Formations: Comparison Between Recurrent and Conventional Neural Networks," Paper presented at the 53rd US Rock Mechanics/Geomechanics Symposium held in New York, NY, USA, 2019.

[2] M. Asoodeh and P. Bagheripour, "Prediction of Compressional, Shear, and Stoneley Wave Velocities from Conventional Well Log Data Using a Committee Machine with Intelligent Systems," Vol. 45, Rock Mechanics and Rock Engineering, 2012, pp. 45-63. doi 10.1007/s00603-011-0181-2.

[3] R. K. Abdul Majeed and A. A. Alhaleem, "Estimation of shear wave velocity from wireline logs data for Amara oilfield, Mishrif formation," Vol. 53, No.1A, Iraqi Geological Journal, 2020. https://doi.org/10.46717/igj.53.1a.R3.2020.01.30.

[4] R. K. Abdul Majeed and A. A. Alhaleem, "An Accurate Estimation of Shear Wave Velocity Using Well Logging Data for Khasib Carbonate Reservoir - Amara Oil Field," Vol. 26, No.6, Journal of Engineering, 2022.

[5] R. H. Allawi and M. S. Al-Jawad, "An Empirical Correlations to Predict Shear Wave Velocity at Southern Iraq Oilfield," No. 34 part 1, Journal of Petroleum Research and Studies, 2022, pp. 1-14.

[6] M. A. Kassab and A. Weller, "Study on P-wave and S-wave velocity in dry and wet sandstones of Tushka region, Egypt," Vol. 24, Egyptian Journal of Petroleum, 2015, pp. 1-11.

[7] Q. A. Abdul-Aziz and H. A. Abdul-Hussein, "Development a Statistical Relationship between Compressional Wave Velocity and Petrophysical Properties from Logs Data for JERIBE Formation ASMARI Reservoir in FAUQI Oil Field," Vol. 22, No. 3, Iraqi Journal of Chemical and Petroleum Engineering, 2022, pp. 1-9.

[8] G. R. Pickett, "Acoustic Character Logs and Their Applications in Formation Evaluation," Vol. 15, No. 6, J Pet Technol, SPE-452-PA, 1963, pp. 659-667.

[9] R. D. Carroll, "The determination of the acoustic parameters of volcanic rocks from compressional velocity measurements," Vol. 6, Int. J. Rock Mech, 1969, pp. 557-579.

[10] J. P. Castagna, M. L. Batzle, and R. L. Eastwood, "Relationships between compressional-wave and shear-wave velocities in clastic silicate rocks," Vol. 50, No.4, Geophysics, 1985.

[11] D. Freund, "Ultrasonic compressional and shear velocities in dry clastic rocks as a function of porosity, clay content, and confining pressure," Vol. 108, Geophys. J. Inr. 1992. pp. 125-135.

[12] H. Eskandari, M. R. Rezaee and M. Mohammadina, "Application of multiple regression and artificial neural network techniques to predict shear wave velocity from wireline log data for carbonate reservoir, South-West Iran," Vol. 42, CSEG Recorder, 2004, pp. 40- 48.

[13] T. M. Brocher, "Empirical Relations between Elastic Wave speeds and Density in the Earth's Crust," Vol. 95, No. 6, Bulletin of the Seismological Society of America, 2005, pp. 2081–2092.

[14] M. S. Ameen, B. G. D. Smart, J. M. Somerville, S. Hammilton and N. A. Naji, "Predicting rock mechanical properties of carbonates from wireline logs (A case study: Arab-D reservoir, Ghawar field, Saudi Arabia)," Vol. 26, Marine and Petroleum Geology, 2009, pp. 430–444.

[15] W. M. Al-Kattan, "Prediction of Shear Wave velocity for carbonate rocks," Vol. 16, No. 4, Iraqi Journal of Chemical and Petroleum Engineering. 2015. pp. 45-49.

[16] M. R. Rezaee, A, K. Ilkhchi and A. Barabadi, "Prediction of shear wave velocity from petrophysical data utilizing intelligent systems: An example from a sandstone reservoir of Carnarvon Basin, Australia," Vol. 55, Journal of Petroleum Science and Engineering, 2007, pp. 201-212.

[17] K. Tabari, O. Tabari and M. Tabari, "A Fast Method for Estimating Shear Wave Velocity by Using Neural Network," Vol. 5, No. 11, Australian Journal of Basic and Applied Sciences, 2011. pp. 1429-1434.

[18] F. A. Hadi and R. Nygaard, "Shear Wave Prediction in Carbonate Reservoirs: Can Artificial Neural Network Outperform Regression Analysis," Paper presented at the 52nd US Rock Mechanics / Geomechanics Symposium held in Seattle, Washington, USA, 2018.

[19] A. Al Ghaithi and M. Prasad, "Machine learning with Artificial Neural Networks for shear log predictions in the Volve field Norwegian North Sea," Society of Exploration Geophysicists. SEG International Exposition and 90th Annual Meeting, 2020.

[20] J. M. Al Said Naji, G. H. Abdul-Majeed, and A. K. Alhuraishawy, " Prediction sonic shear wave by artificial neural network," Vol.55 (2E), pp.152-164, Iraqi geological journal, 2022.

[21] Q. A. Abdul-Aziz and H. A. Abdul-Hussein, "Integration of Geomechanical and Petrophysical properties for estimating rate of penetration in Fauqi oil field Southern Iraqi," Doctorate dissertation, University of Baghdad, Collage of Engineering, Iraq, 2021.

[22] W. I. Taher, M. S. Al Jawad and C. W. V. Kirk, "Reservoir study for Asmari reservoir/Fauqi field," Master thesis, University of Baghdad, Collage of Engineering, Iraq, 2011.

[23] J. E. Fox and T. S. Ahlbrandt, "Petroleum Geology and Total Petroleum Systems of the Widyan Basin and Interior Platform of Saudi Arabia and Iraq. U.S," Geological Survey Bulletin, 2002.

[24] Z. Tariq, S. Elkatatny, M. Mahmoud and A. Abdulraheem, "A New Artificial Intelligence Based Empirical Correlation to Predict Sonic Travel Time," Paper presented at the International Petroleum Technology Conference, IPTC-19005-MS, 2016.

[25] S. Maleki, A. Moradzadeh,R. G. Riabi, R. Gholami and F. Sadeghzadeh, "Prediction of shear wave velocity using empirical correlations and artificial intelligence methods," Vol. 3, NRIAG Journal of Astronomy and Geophysics, 2014, pp. 70-81.

[26] H. Akhundi, M. Ghafoori and G. R. Lashkaripour, "Prediction of Shear Wave Velocity Using Artificial Neural Network Technique, Multiple Regression and Petrophysical Data: A Case Study in Asmari Reservoir (SW Iran)," Vol. 4, Open Journal of Geology, 2014, pp. 303-313.

[27] E. Jorjani, C. S. Chehreh and S. H. Mesroghli, "Application of artificial neural networks to predict chemical desulfurization of Tabas coal," Vol. 87, Fuel, 2008, pp. 2727–3273.

[28] G. H. Abdul-Majeed, F.S. Kadhim, F. H. Almahdawi, Y. Al-Dunainawi, A. Arabi and W. K. Al-Azzawi, "Application of artificial neural network to predict slug liquid holdup," Vol. 150. International Journal of Multiphase Flow, 2022.

[29] M. A. Razavi, A. Mortazavi and M.Mousavi, "Dynamic modeling of milk ultrafiltration by artificial neural network," Vol. 120, J. Membrane. 2003, pp. 47-58.

مقارنة في تخمين زمن موجة القص الصوتية بأستخدام المعادلات التجريبية والشبكة العصبية الاصطناعية

جاسم محمد السيد ناجي [١], غسان حميد عبد المجيد [٢], و علي خيون الحريشاوي [٣]

[١] جامعة بغداد, كلية الهندسة, قسم هندسة النفط, بغداد, العراق.
[٢] جامعة بغداد, بغداد, العراق.
[٣] وزارة النفط, دائرة المكامن وتطوير الحقول, بغداد, العراق.

الخلاصة

نمذجة ثبوتية البئر والتنبأ بأنتاج الرمل تتأثر جدا بزمن موجة القص الصوتية. في اي حقل لا يتوفر زمن موجة القص الصوتية لكل الآبار نسبة لكلف قياسه العالية. العديد من الباحثين طوروا معادلات تجريبية بأستخدام بيانات بعض الحقول العالمية لحساب زمن موجة القص الصوتية. مؤخرا استخدم الباحثون طرق الذكاء الاصطناعي لحساب زمن موجة القص الصوتية. ثلاث طرق تجريبية موجودة لكل من كارول وفريوند وبرونشر تم استخدامها لحساب زمن موجة القص الصوتية في هذا البحث, بينما الرابعة تم تطويرها. للمقارنة مع نتائج المعادلات التجريبية المستخدمة تم استخدام نتائج دراسة استخدمت فيها الشبكة العصبية الاصناعية لحساب زمن موجة القص الصوتية. نفس البيانات المستخدمة في دراسة الشبكة الاصطناعية تم اعتمادها هنا حيث تشتمل هذه البيانات على ١٩٢٢ نقطة مقاسة من عمليات الجس لزمن موجة القص الصوتية مع قياسات تسعة مجسات تشمل مجس اشعة كاما ومجس زمن الموجة الصوتية الانضغاطية ومجس قطر البئر ومجس النيوترون ومجس الكثافة ومجس المقاومية العميقة بالاضافة لقراءات زاوية ميل البئر وزاوية الميل عن الشمال والعمق الشاقولي لبئر اتجاهي عراقي. المعادلات التجريبية الثلاث الموجودة تستند في حساب زمن موجة القص الصوتية على نقاط قياسات ازمان الموجات الصوتية الانضغاطية. المعادلة التجريبية الرابعة تم تطويرها باستخدام كل النقاط المقاسة لازمان موجات القص والانضغاط الصوتيتان. المقارنة بين الطرق وضحت ان طريقة الشبكة العصبية الاصطناعية كانت الافضل بأعلى معامل ترابط مساوي ل ٠,٩٦٦ واقل عوامل احصائية اخرى بالمقارنة مع الطرق التجريبية الاربع حيث ان معامل ترابط المعادلات التجريبية لكل من كارول وفريوند وبرونشر والمعادلة المطورة الرابعة كان ٠,٧٨٢٦ و ٠,٧٦٣٦ و ٠,٦٧٦٤ و٠,٨٠١٦ على التوالي بالاضافة الى بقية المعاملات الاحصائية التي اثبتت ان المعادلة التجريبية المطورة افضل من الثلاث الموجودات. استخدام طريقة الشبكة الاصطناعية او المعادلة التجريبية المطورة مستقبلا لحساب زمن موجة القص الصوتية متعلق بصانعي القرار نسبة لعدد من المحددات ودقة نتائج موجة القص الصوتية المستهدفة.

الكلمات الدالة: المعادلات التجريبية, الشبكة العصبية الاصطناعية, موجة القص الصوتية, انحراف حفرة البئر, زاوية ميل البئر وزاية الانحراف عن الشمال.